

# **SANDIA REPORT**

SAND2001-3416

Unlimited Release

Printed November 2001

## **Sandia SCADA Program Real-Time Feedback Control of Power Systems**

Anthony E. Bentley, Jason E. Stamp, Rolf E. Carlson

Prepared by  
Sandia National Laboratories  
Albuquerque, New Mexico 87185 and Livermore, California 94550

Sandia is a multiprogram laboratory operated by Sandia Corporation,  
a Lockheed Martin Company, for the United States Department of  
Energy under Contract DE-AC04-94AL85000.

Approved for public release; further dissemination unlimited.



**Sandia National Laboratories**

Issued by Sandia National Laboratories, operated for the United States Department of Energy by Sandia Corporation.

**NOTICE:** This report was prepared as an account of work sponsored by an agency of the United States Government. Neither the United States Government, nor any agency thereof, nor any of their employees, nor any of their contractors, subcontractors, or their employees, make any warranty, express or implied, or assume any legal liability or responsibility for the accuracy, completeness, or usefulness of any information, apparatus, product, or process disclosed, or represent that its use would not infringe privately owned rights. Reference herein to any specific commercial product, process, or service by trade name, trademark, manufacturer, or otherwise, does not necessarily constitute or imply its endorsement, recommendation, or favoring by the United States Government, any agency thereof, or any of their contractors or subcontractors. The views and opinions expressed herein do not necessarily state or reflect those of the United States Government, any agency thereof, or any of their contractors.

Printed in the United States of America. This report has been reproduced directly from the best available copy.

Available to DOE and DOE contractors from  
U.S. Department of Energy  
Office of Scientific and Technical Information  
P.O. Box 62  
Oak Ridge, TN 37831

Telephone: (865)576-8401  
Facsimile: (865)576-5728  
E-Mail: [reports@adonis.osti.gov](mailto:reports@adonis.osti.gov)  
Online ordering: <http://www.doe.gov/bridge>

Available to the public from  
U.S. Department of Commerce  
National Technical Information Service  
5285 Port Royal Rd  
Springfield, VA 22161

Telephone: (800)553-6847  
Facsimile: (703)605-6900  
E-Mail: [orders@ntis.fedworld.gov](mailto:orders@ntis.fedworld.gov)  
Online order: <http://www.ntis.gov/ordering.htm>



SAND2001-3416  
Unlimited Release  
Printed November 2001

## **Sandia SCADA Program**

# **Real-Time Feedback Control of Power Systems**

Anthony E. Bentley  
Control Subsystems

Jason E. Stamp  
Networked Systems Survivability & Assurance

Rolf E. Carlson  
Advanced Information & Control Systems

Sandia National Laboratories  
P.O. Box 5800  
Albuquerque, New Mexico 87185-0455

### **Abstract**

This report documents work supporting the Sandia National Laboratories initiative in Distributed Energy Resources (DERs) and Supervisory Control and Data Acquisition (SCADA) systems. One approach for real-time control of power generation assets using feedback control, Quantitative feedback theory (QFT), has recently been applied to voltage, frequency, and phase-control of power systems at Sandia. QFT provided a simple yet powerful philosophy for designing the control systems—allowing the designer to optimize the system by making design tradeoffs without getting lost in complex mathematics. The feedback systems were effective in reducing sensitivity to large and sudden changes in the power grid system. Voltage, frequency, and phase were accurately controlled, even with large disturbances to the power grid system.

# CONTENTS

Introduction .....	5
Feedback Control Design Techniques .....	5
QFT Application .....	8
Frequency Control.....	14
Conclusions .....	20

## Figures

Figure 1. Three-Phase Power System Simulation Diagram with Load Disturbances .....	9
Figure 2. Simulation Results from Figure 1.....	9
Figure 3. Power System Simulation for Connecting a Slave Power Plant to a Power Grid.....	10
Figure 4. Simulation Results of Phase Control from Figure 3.....	11
Figure 5. Voltage Control from Figure 3.....	11
Figure 6. Simulation Results from Figure 4.....	12
Figure 7. Bode Plots of the Open-Loop Voltage Control Plant $V(s)$ with Compensator $G_1(s)$ and Feedback Sensor $H(s)$ . $L(s) = G_1(s) \cdot V(s) \cdot H_1(s)$ .....	13
Figure 8. Bode Plots of Closed-Loop Voltage Regulator $T(s)$ .....	14
Figure 9. Bode Plots of Open-Loop Frequency Controller.....	15
Figure 10. Bode Plot of Closed-Loop Frequency Control.....	16
Figure 11. Bode Plot of Open-Loop Phase Controller.....	17
Figure 12. Nichols Plots of Uncompensated Phase Control System.....	18
Figure 13. Nichols Plot of Compensated Phase Controller.....	18
Figure 14. Bode Plot of Closed-Loop Phase Controller.....	19

## Table

Table 1. Four Categories of Feedback Control Design Techniques .....	5
----------------------------------------------------------------------	---

## Introduction

This report documents work supporting the Sandia National Laboratories initiative in Distributed Energy Resources (DERs) and Supervisory Control and Data Acquisition (SCADA) systems. SCADA systems are information systems that provide the command and control capability necessary to manage the nation’s critical infrastructures such as the power grid, and they are also critical in managing distributed energy resources such as microturbines, solar, and wind farms. In understanding the requirements and constraints on future DER SCADA systems, it is necessary to understand the information needed to effectively and efficiently manage DER assets. One area in DER that is evolving is real-time control of DER generators to safely and economically take units on and off line. This study looked at one approach, Quantitative Feedback Theory, for real-time control of power generation assets using feedback control.

## Feedback Control Design Techniques

Most feedback control design techniques can be divided into four basic categories: (1) classical-empirical, (2) modern-empirical, (3) classical-analytical, and (4) modern-analytical. Table 1 shows several feedback control design techniques and groups them into one of the four categories:

**Table 1. Four Categories of Feedback Control Design Techniques**

	<b>Classical</b>	<b>Modern</b>
<b>Empirical</b>	Proportional Integral Derivative (PID) and Bang-Bang	Fuzzy Logic, Neural Networks and Adaptive
<b>Analytical</b>	Bode, Root-Locus, Linear Quadratic Regulator and Gaussian (LQR & LQG)	$H^2$ , $H^\infty$ , Lyapunov and Quantitative Feedback Theory (QFT)

*Empirical* techniques are those that do not rely on accurate models of the plants to be controlled. For these techniques, it is possible to develop working controllers with minimum knowledge about the plant—by treating the plant as a “black-box.” For example, PID control is typically implemented by manually adjusting the three gains—(1) proportional, (2) integral, and (3) derivative—until the desired response is achieved. Bang-Bang control is typically applied to processes that have very long time-constants relative to the sample rate of the controller. Under these conditions, Bang-Bang control produces inherently stable designs (e.g., heating and cooling systems).

Modern applications of empirical design attempt to bring the sophistication of high-speed computers into the design process. Fuzzy Logic extends the Bang-Bang control technique to allow more than two states (“off” and “on”) by means of various levels of the “on” state. Essentially, Fuzzy Logic is a digital approximation for analog control. Neural Networks and

*adaptive* techniques are significantly more complicated approaches, which, under the right conditions, can accurately emulate the dynamic behavior of a plant. These sophisticated plant models can then be used to linearize and/or cancel out undesirable behaviors in the plant.

A major limitation of empirical design is that it does not produce analytical data for quantifying design margins. That is, acceptable performance of the system over a wide range of plant uncertainty, time variance, and/or nonlinearity cannot be rigorously proven. Stability can only be demonstrated by testing the system over the expected range of plant uncertainty. Engineers often spend more time tuning feedback parameters than understanding the process they want to control. The power of ordinary feedback—even when designed empirically—is so tremendous that impressive benefits are achieved in the laboratory by such designs once they have been carefully tuned. However, empirically designed feedback systems have often caused more uncertainty in the processes they are trying to control when they are implemented on the factory floor. As a result, feedback control has developed a bad reputation throughout the industrial community.

Dr. W. Edwards Deming, the internationally renowned consultant whose work directly led Japanese industry to revolutionize its quality and productivity, said the following about feedback control: “Gadgets and servomechanisms that by mechanical or electronic circuits guarantee zero defects will destroy the advantage of a beautiful narrow distribution of dimensions. They slide the distribution back and forth inside the specification limits, achieving zero defects and at the same time driving losses and costs to the maximum.”<sup>1</sup>

In contrast to empirical design are the analytical or theoretical approaches to feedback design, which use mathematically rigorous theorems to guarantee the performance of the feedback system to quantifiable performance objectives. Classical-analytical design theories include *Bode*, *Root-locus*, *Linear Quadratic Regulator (LQR)*, and *Linear Quadratic Gaussian (LQG)*. These and other classical theories have one caveat: they assume that the plant to be controlled is linear and time invariant. While these techniques are often successfully applied to nonlinear and time-variant systems, the classical theories do not rigorously apply to these rogue systems. That is, these classical theories (as originally formulated) cannot guarantee acceptable performance of the feedback system over a large range of plant uncertainty. This is unfortunate because most industrial processes are highly nonlinear, time-variant systems.

Finally, there are the modern extensions of feedback control theory, such as  $H^2$  and  $H^\infty$ . These techniques attempt to address the issue of plant uncertainty. As pointed out by Dr. Isaac Horowitz, the purpose of feedback control is to handle uncertainty.<sup>2</sup> About 1963, Dr. Horowitz

---

<sup>1</sup> W. Edwards Deming, *Out of the Crisis*. Massachusetts Institute of Technology Center for Advanced Engineering Study, Cambridge, MA, 1982 pp. vii, 141-142. (In recognition of Dr. Deming’s “contribution to the economy of Japan,” the Union of Japanese Science and Engineering now gives annual prizes in his name for contributions to product quality and dependability. In 1960, the emperor of Japan awarded him the Second Order Medal of the Sacred Treasure. Dr. Deming has also received numerous other awards, including the Shewhart Medal from the American Society for Quality Control in 1956 and the Samuel S. Wilks Award from the American Statistical Association in 1983.

<sup>2</sup> Isaac Horowitz, *Synthesis of Feedback Systems*. Academic Press, New York, 1963.

called attention to the fact that if a system is perfectly linear and time-invariant with no uncertainty, then there is no need for feedback, and the desired performance can more easily be achieved through feed-forward techniques. While  $H^2$  and  $H^\infty$  theory address plant uncertainty, they also constrain the plant to linear, time-invariant systems. This is a serious disadvantage for industrial feedback applications because most real-world systems are nonlinear. To address nonlinear plants, the feedback engineer either turns to the complicated Lyapunov technique or attempts to linearize the plant about some nominal operating point. While linearization allows the designer to obtain acceptable performance near the linearization point, there is no rigorous proof of acceptable performance outside of the region of linearization.

As a result, most industrial engineers find modern control theories too theoretical for their backgrounds<sup>3</sup> and typically resort to empirical methods of feedback design. This regrettable situation has led to some strong statements such as, “In developing [process] control, system theory is not of much help.”<sup>4</sup>

One explanation for this impression prevalent among industrial engineers has to do with the complicated dynamics of most industrial processes that are seldom linear and time-invariant with no uncertainty. Modern analytical control methods require some form of plant model with a very generalized uncertainty structure. Though it is possible to derive such models from experimental data, the time it takes to derive such meaningful descriptions is usually prohibitive. In addition, modern control design methods typically result in overly conservative controllers, which require the engineer to reevaluate the plant model. This design-by-iteration process, a fact of life in real-world applications, must be as short as possible.

Contrasting the prevalent modern control methods in terms of its applicability to industrial processes is Quantitative Feedback Theory (or QFT). QFT is a rigorous engineering design method for robust performance specifications that is applicable to large classes of nonlinear and/or time-varying systems, as well as to linear systems. QFT is a valuable tool for the following reasons: (1) it does not require identification of plant dynamics with uncertainty models—can use input/output data directly without fitting the data to mathematical models; (2) it employs classical frequency domain concepts with which most engineers are familiar, but it is emphasized that QFT is nevertheless mathematically precise (no approximations), for large classes of highly uncertain nonlinear time-varying plants; and (3) the design process is highly transparent so that the “cost of feedback” in terms of compensator complexity, gain and bandwidth, number of sensors needed, sensor accuracy, sensor noise effects, and design effort are clearly seen by the engineer, empowering him or her to make the necessary performance tradeoffs throughout the design cycle.

---

<sup>3</sup> Manfred Morari, Control Theory and Process Control Practice, Plenary Session 2, American Control Conference, Boston, June 28, 1991.

<sup>4</sup> B. W. Schumacher, J. C. Cooper, and W. Dilay, Resistance Spot Welding Control That Automatically Selects the Welding Schedule for Different Types of Steel. *Society of Automotive Engineers Technical Paper Series*, 850407 (1985).

If an accurate model (including uncertainty) does exist of the nonlinear plant, one can design the closed loop system to meet predefined performance specifications.<sup>5,6</sup> Another great advantage of QFT is that it allows the engineer to apply feedback theory to a wide variety of complex, ill-behaved systems\*, without requiring extensive new design skills. The same techniques learned in classical control theory can be reapplied to complicated and challenging systems—thus liberating the engineer to concentrate on conflicting design requirements and control strategies, rather than learning new mathematics. For example, QFT has been successfully applied to various welding processes at Sandia National Laboratories. In each case, the “robustness” of the welding process was tremendously improved—far above results of any work previously published.<sup>7,8</sup> Essentially, QFT has all the advantages of the less-complicated classical design techniques such as Bode but has none of the limitations of classical or other modern control techniques.

## QFT Application

QFT has recently been applied to voltage, frequency, and phase-control of power systems at Sandia. These systems have been designed and tested on a simulated power grid to achieve

- RMS voltage control to  $\pm 6\%$  of nominal with  $+1000\%$  /  $-50\%$  load disturbances (Figures 1 and 2).
- Frequency control to  $\pm 0.35\%$  of nominal with  $+1000\%$  /  $-50\%$  load disturbances (Figures 1 and 2).

A synchronization control algorithm was also designed and tested for synchronizing and connecting multiple power plants onto a grid. (See Figures 3, 4 and 5.) To connect a power plant to the grid, both the voltage and phase of the plant must match what is on the grid at the point of connection. Once these are matched, the power plant is connected. When the plant is first connected, it is not generating power; it is simply running at synchronous speed.

---

<sup>5</sup> Isaac Horowitz and M. Sidi, "Synthesis of Feedback Systems with Large Plant Ignorance of Prescribed Time Domain Tolerances," *International Journal of Control*, vol. 16, pp. 187-309, (1972).

<sup>6</sup> Isaac Horowitz, *Quantitative Feedback Design Theory*, vol. 1. QFT Publications, Boulder, CO, 1993, Chapter 11.

\* Such as unstable and/or nonminimum phase plants (time delays), multiple-loop plants with a variety of available internal sensing points—how to divide up the feedback burden between them, multiple-input multiple-output plants (e.g., in a 3-by-3 plant, the nine closed-loop system response functions to commands and disturbances can be individually controlled despite large uncertainties).

<sup>7</sup> A. E. Bentley, "Quantitative Feedback Theory with Applications in Welding." *International Journal of Robust and Nonlinear Control*, vol. 4, issue 1, January 1994.

<sup>8</sup> A. E. Bentley, *Control of Resistance Plug Welding Using Quantitative Feedback Theory*. SAND94-0795A. Sandia National Laboratories, Albuquerque, NM.



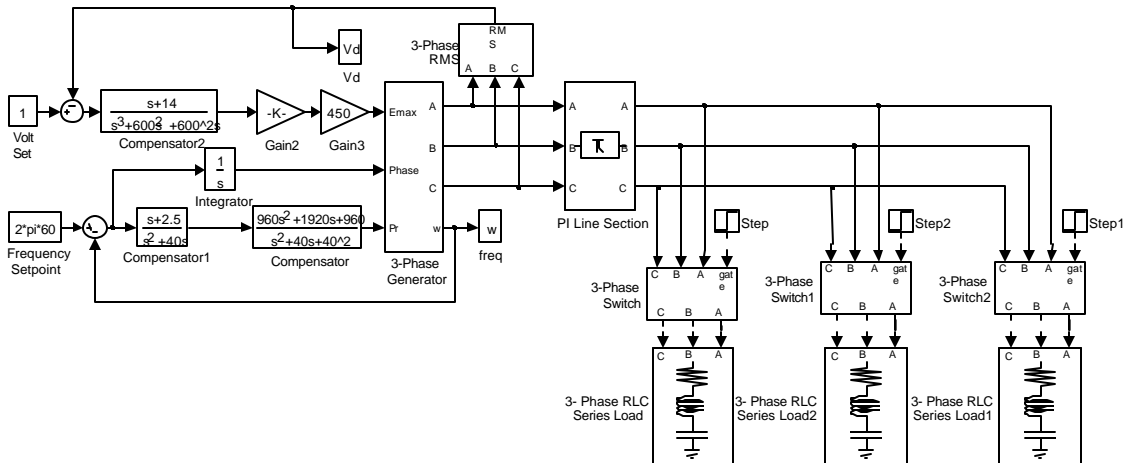


**Figure 1. Three-Phase Power System Simulation Diagram with Load Disturbances.** (The nominal load consists of 4.2 p.u. W resistance with a series inductance of 6 p.u. mH. At t=5 seconds, the resistance is instantly switched to 42 p.u. W, the inductance is switched to 12 p.u. mH, and a series capacitor of 10 p.u. F is also added. At t=10 seconds, a parallel load is instantly added with resistance of 2 p.u. W and series inductance of 3 p.u. mH. Results of this simulation are shown in Figure 2.)

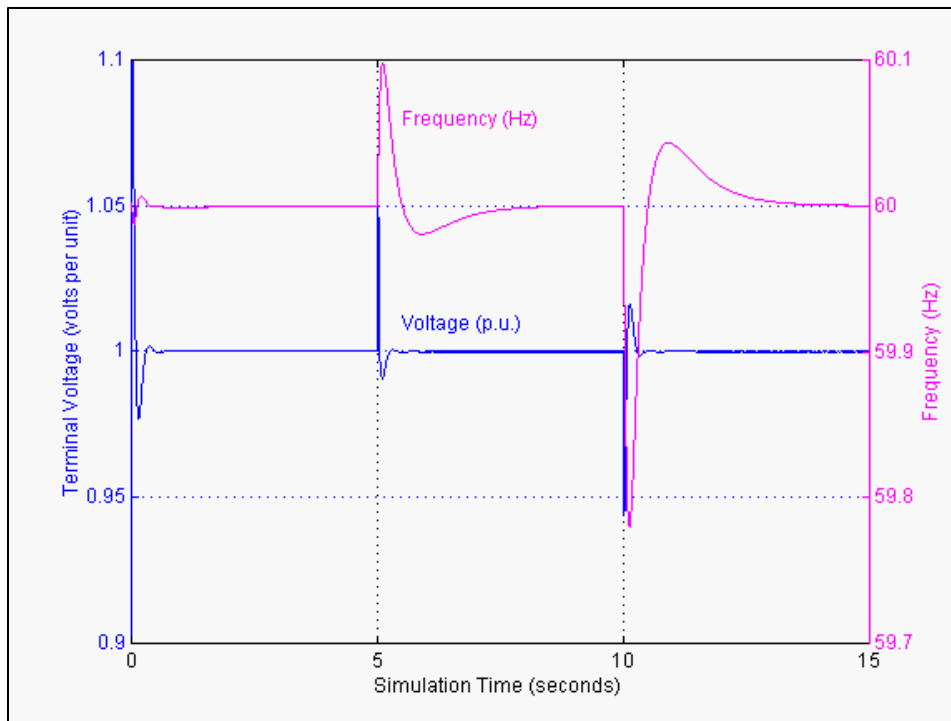


**Figure 2. Simulation Results from Figure 1.** (Nominal terminal voltage is 1 volt per unit.)

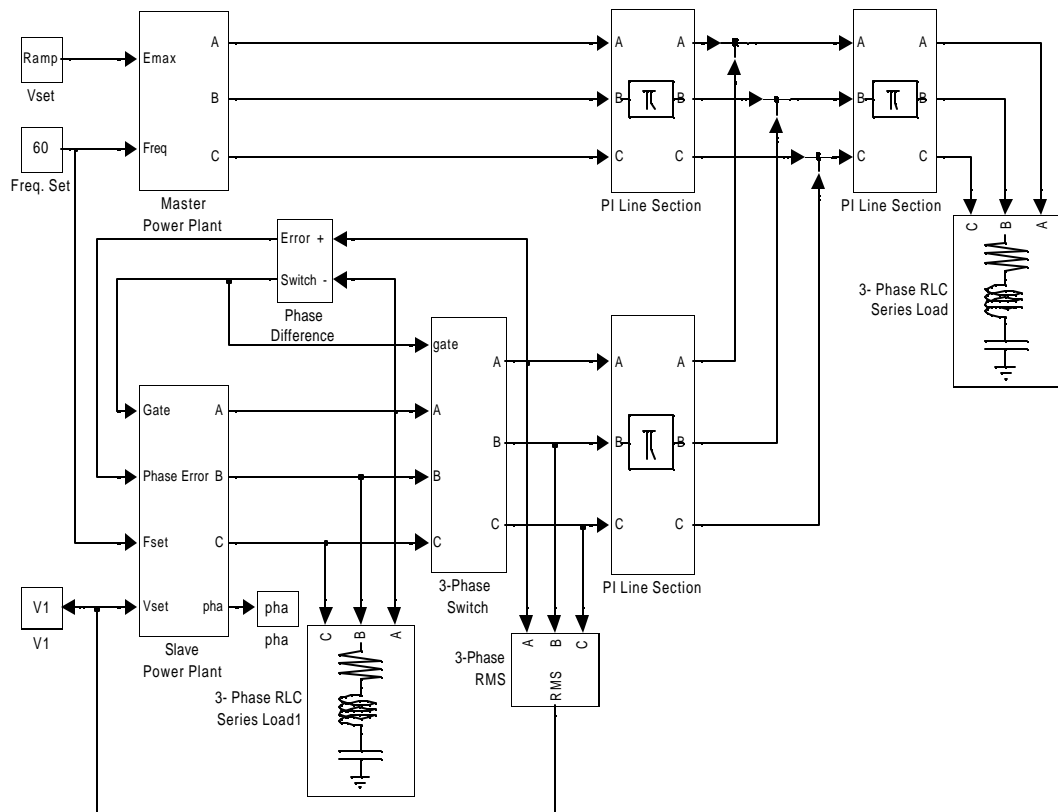


**Figure 3. Power System Simulation for Connecting a Slave Power Plant to a Power Grid. (The phase shift across the three-phase switch is forced to zero by adjusting the phase of the slave power plant. The power plant voltage is also adjusted to match the line voltage at the switch. When both the phase and the voltage are matched, the three-phase switch is closed—connecting the slave power plant to the grid.)**

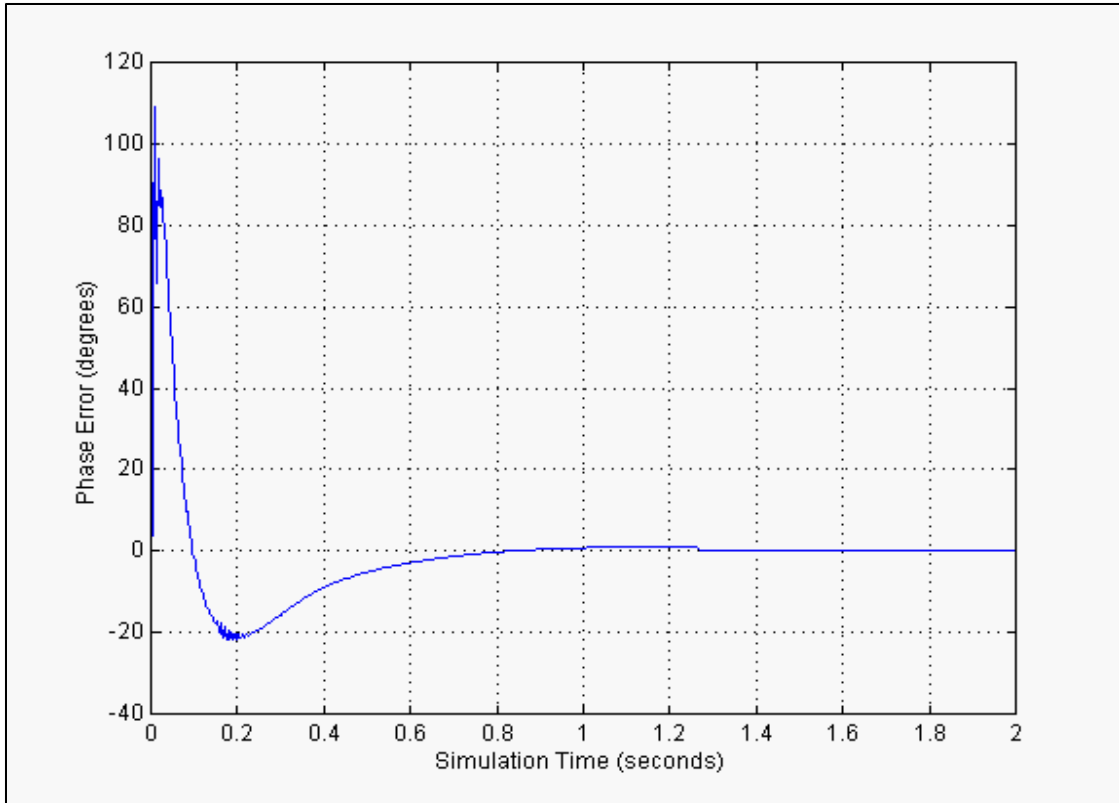


Figure 4. Simulation Results of Phase Control from Figure 3. (At t=1.25 seconds the slave power plant is connected to the grid.)

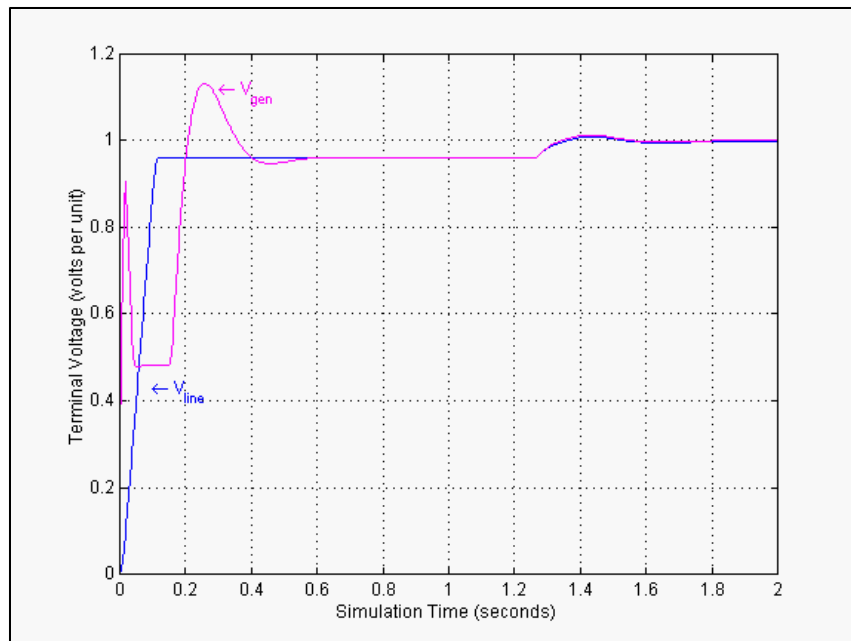


Figure 5. Voltage Control from Figure 3. (At t=1.25 s, the slave power plant is connected to the grid.)

Power control (phase control) for a plant connected to a power system grid was also designed and successfully tested. Once the power plant has been connected to the grid, the voltage control set point is increased to 1 volt per unit to keep the grid voltage within specification. The phase of the power plant is also increased after it is connected so that the power plant begins to push power onto the grid—rather than just running at synchronous speed without adding power (Figure 6).

The design of these controllers using QFT is briefly discussed below. The terminal voltage of the power supply is given in Laplace format as

$$V(s) = \frac{k}{s+a} \quad \text{where } 0.75 \leq k \leq 1 \text{ and } 0.8 \leq a \leq 1.2.$$

The output of  $V(s)$  is also limited between 0.7 and 2.0. The root-mean-square of the voltage is measured and feedback to the voltage controller. This feedback sensor is characterized in the Laplace domain as

$$H_1(s) = \frac{e^{-st}}{st} \quad \text{where } t = \frac{1}{60} \text{ second.}$$

The compensator for the voltage control system was designed using QFT as shown below:

$$G_1(s) = \frac{k(s+a)\mathbf{w}^2}{a(s^2 + 2z\mathbf{w}s + \mathbf{w}^2)} \quad \text{where : } k = 450, a = 14, \mathbf{w} = 600 \text{ and } z = 0.5.$$

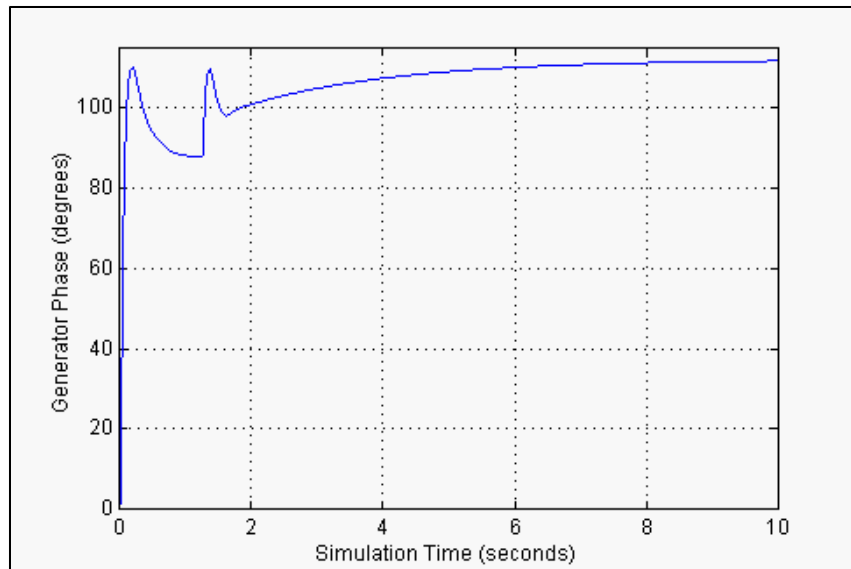


**Figure 6. Simulation Results from Figure 3. Once the slave power plant has been connected to the grid (at  $t=1.25$  seconds), the phase control set point is advanced somewhat so that the power plant begins to push power onto the grid.**

Because of load uncertainty in the power grid, the gain  $k$  is uncertain, as well as the time constant  $a$ . Thus, a family of plant equations that spans the range of uncertainty in the system is used to represent the voltage control system rather than using a single equation. The open-loop system  $L(s) = G_1(s) \cdot V(s) \cdot H_1(s)$  is shown in Figure 7 in the format of a Bode plot of compensated plant equations  $L(s)$ . Note that the system has a phase margin of at least  $65^\circ$  and a gain margin of at least 10 dB for all plants in the set.

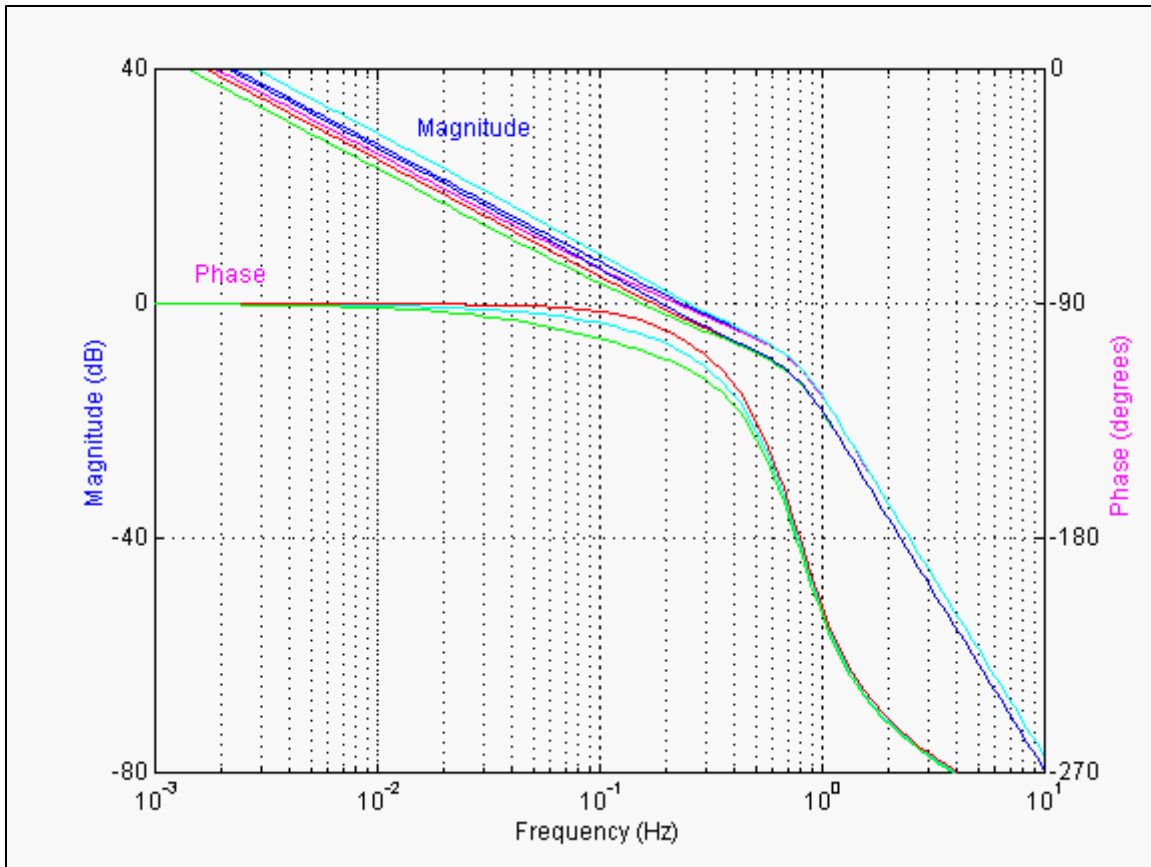


**Figure 7. Bode Plots of Open-Loop Voltage Control Plant  $V(s)$  with Compensator  $G_1(s)$  and Feedback Sensor  $H(s)$ .  $L(s) = G_1(s) \cdot V(s) \cdot H_1(s)$ .**

The transfer function for the closed-loop or regulated voltage control system is given by

$$T(s) = \frac{G_1(s)V(s)}{1 + G_1(s)V(s)H_1(s)}$$

The closed-loop voltage controller  $T(s)$  is plotted in Figure 8. Note the effect of feedback on the system uncertainty: for frequencies below the system bandwidth, the uncertainty has essentially been eliminated. At higher frequencies, where system uncertainty is less important, the uncertainty is the same as for the open-loop system.

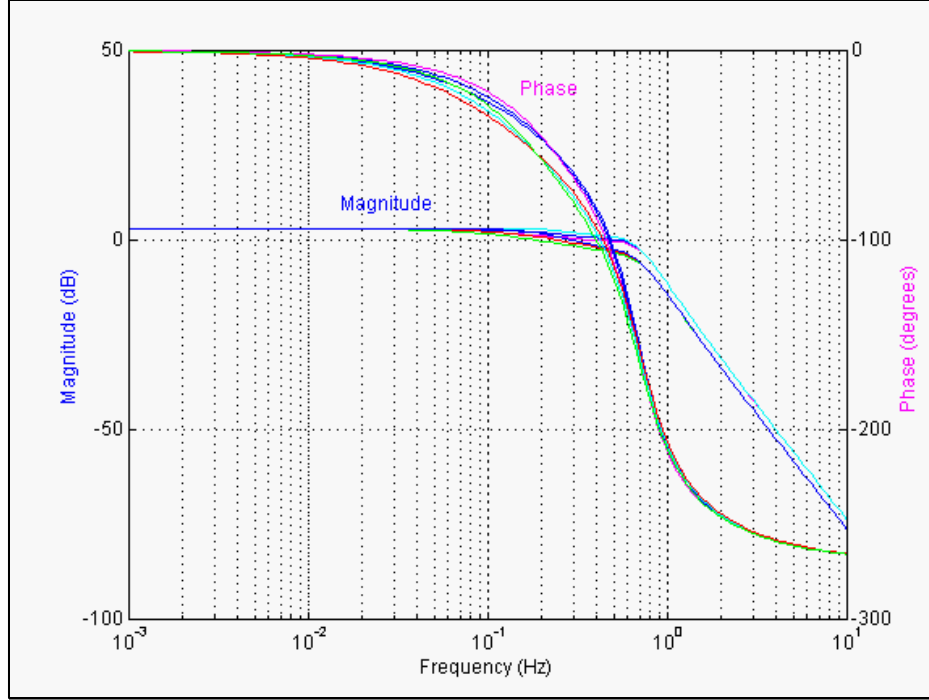


Figure 8. Bode Plots of Closed-Loop Voltage Regulator  $T(s)$ .

## Frequency Control

The frequency control for the system was also designed using QFT. The system consists of a mechanical power source  $F(s)$ , which converts power in (such as fuel) to output torque. The torque is then applied to the plant  $P_1(s)$  that converts torque into frequency.  $H_2(s)$  takes the frequency output of  $P(s)$  and converts it to electrical power. Because of the power source  $F(s)$ , the system has a much slower time constant than that of the voltage control system:

$$P_1(s) = \frac{60p}{6.5s}; \quad F(s) = \frac{100a}{(s+a)(bs+1)} \quad \text{where } 1.6 \leq a \leq 2.4 \text{ and } 16 \leq b \leq 24.$$

The transfer function  $H_2(s)$  that converts frequency into “power converted” or power supplied to the grid is actually a nonlinear, time-variant, multiple-input system. The inputs to  $H_2(s)$  include terminal voltage, current, and frequency. The output of  $H_2(s)$  is defined as the instantaneous sum of the product of voltage and current for each of the three phases in power supply and is dependent on the load on the grid. That is,

$$h_2(t, f) = v_{f1}(t, f) \times I_{f1}(t, f) + v_{f2}(t, f) \times I_{f2}(t, f) + v_{f3}(t, f) \times I_{f3}(t, f).$$

In the above equation,  $\mathbf{f}$  is the frequency of the power system. Since current depends on the load and load conditions can also cause disturbances to the frequency, the dynamics of  $h_2(t)$  depends on the conditions on the grid—making  $H_2(s)$  a nonlinear, time-varying system, with large

uncertainties. However, these ill-behaved characteristics of our system can easily be accounted for using QFT. As with uncertainty, nonlinearity and time variance can be rigorously quantified using a *set* of linear, time-invariant equations or plants that fully characterizes the system  $H_2(s)$  over its entire range of nonlinearity, time variance, and uncertainty. The set of equations is shown in the compensated frequency control Bode plots of Figure 9. Figure 9 shows the family of equations that represents the open-loop transfer function of the frequency control system. (Two different compensators  $G_2(s)$  and  $G_3(s)$  were explored for frequency control. The  $G_3(s)$  compensator was used in Figure 9.) Note that, all the plants in the system have at least  $65^\circ$  of phase margin and a conditionally stable gain margin of at least  $+20/-15$  dB. Figure 10 shows the closed-loop feedback system. Also note the large decrease in uncertainty at low frequency because of feedback control (more than 30 dB in the open-loop system at  $f=0.001$  Hz is cancelled out in the closed-loop system).

$$G_2(s) = \frac{960(s+2.5)(s^2+2s+1)}{s(s+40)(s^2+40s+40^2)} \quad G_3(s) = \frac{480,000(s+2)(s^2+4s+4^2)}{s(s+200)(s^2+200s+200^2)}$$

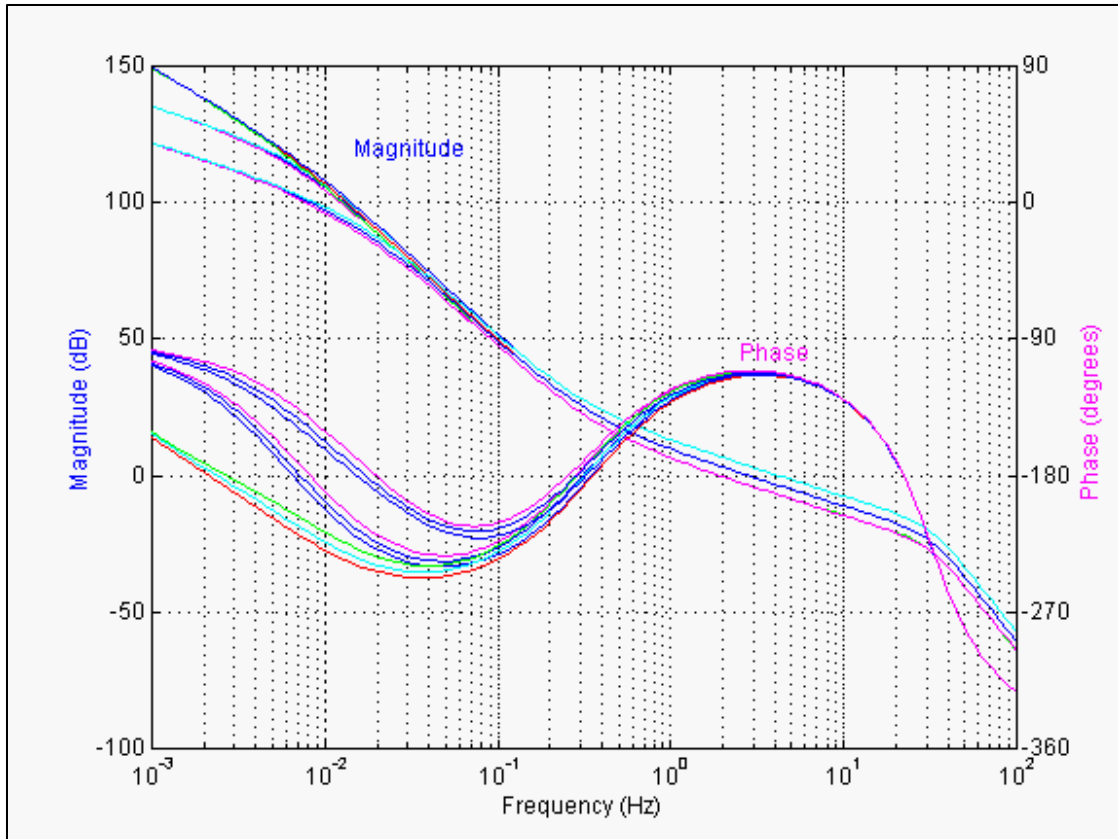
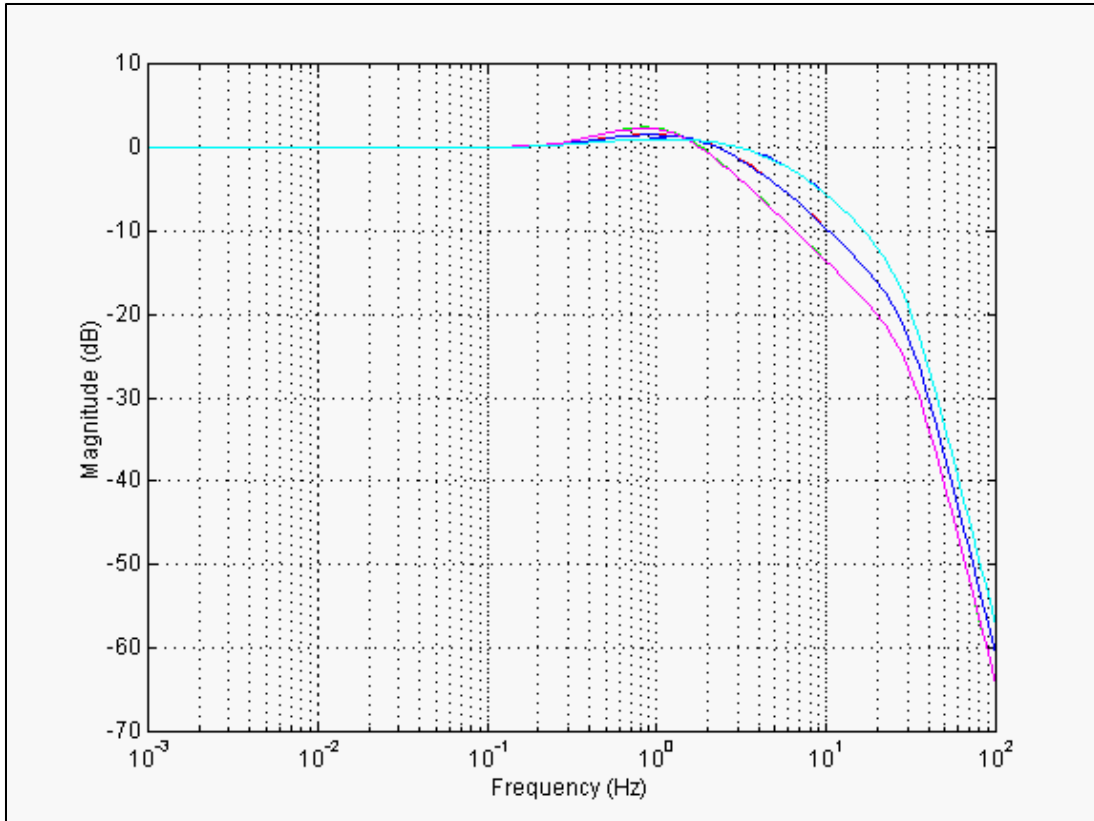


Figure 9. Bode Plots of Open-Loop Frequency Controller.



**Figure 10. Bode Plot of Closed-Loop Frequency Control.**

The phase controller uses almost the same compensator used for frequency control. The only difference is as follows. Phase is defined as the integral of frequency. In terms of Laplace, the phase-control plant  $P_2(s)$  is equal to the frequency control plant  $P_1(s)$  multiplied by  $1/s$ ; that is,  $P_2(s) = P_1(s)/s$ . Because of this extra integrator in the system plant, the integrator in the frequency control compensator  $G_3(s)$  is not used for phase control.

The phase controller is used in the slave power plant to match the frequency and phase of the power grid. At the same time, the voltage controller servos the slave plant to match the voltage of the grid. Once both the voltage and phase are matched, the three-phase switch connects the slave power plant to the power grid. At this point, the dynamics of the plant change considerably. When the plant is first connected, it is not actually generating any power; it is simply spinning at the right frequency to match the grid. After being connected, the phase of the slave plant is advanced to cause the plant to “push” power onto the grid. Because of the “inertia” of the grid, its loads, and other generators, the phase control plant becomes a highly underdamped system with a resonance at about 1.5 Hz. When considering the nonlinearities and uncertainties of the system, this becomes a very challenging system to control using conventional feedback control design techniques. However, using QFT greatly simplified the design for the phase controller.

The open-loop Bode plots for the phase controller are shown in Figure 11. Because of the underdamped resonance at 1.5 Hz together with other plant uncertainty, it is difficult to read the gain and phase margin from the Bode plots in Figure 12. A preferable tool is thus employed in



QFT design, namely, the Nichols plot. The Nichols plot contains the same information as does a Bode plot but uses a more useful format (see Figures 12 and 13). Rather than plotting magnitude and phase vs frequency, the Nichols plot shows phase vs magnitude as the frequency is varied from zero to infinity. When using the Nichols plot to design feedback systems, the Nyquist criterion is satisfied by ensuring that the system crosses the 0 dB gain threshold “to the right” of the  $-180^\circ$  phase threshold. Quantitative design margins can be assured by staying away from the closed-loop magnitude contours that concentrically surround the 0 dB,  $-180^\circ$  instability point. Note that the uncompensated phase control system shown in Figure 12 violates the Nyquist criterion.

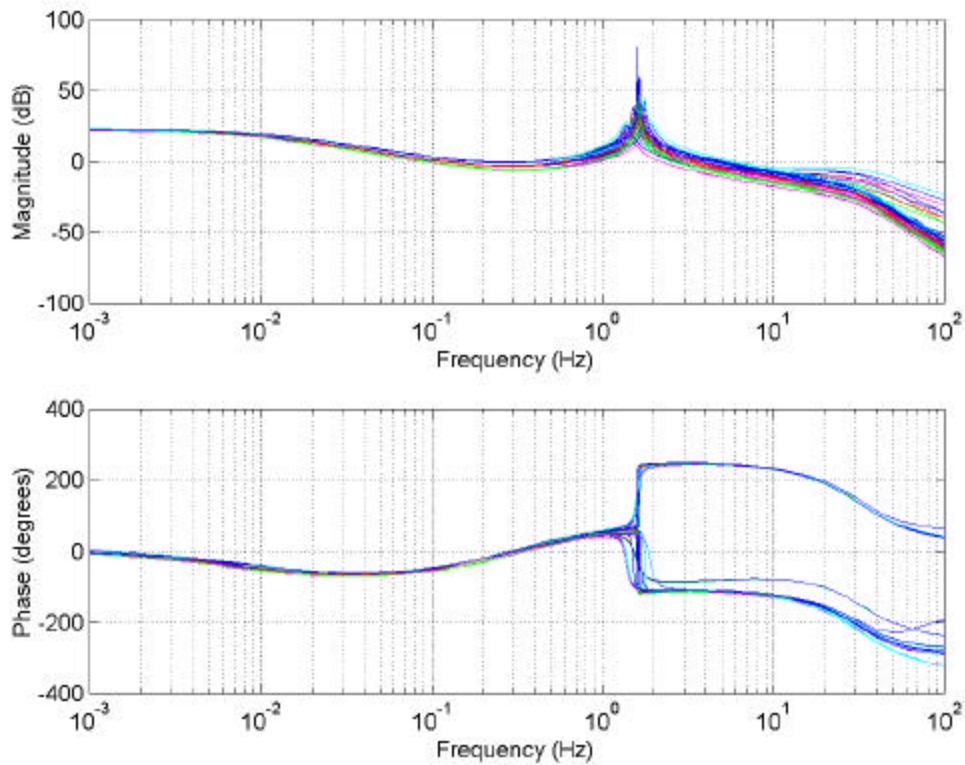


**Figure 11. Bode Plot of Open-Loop Phase Controller.**

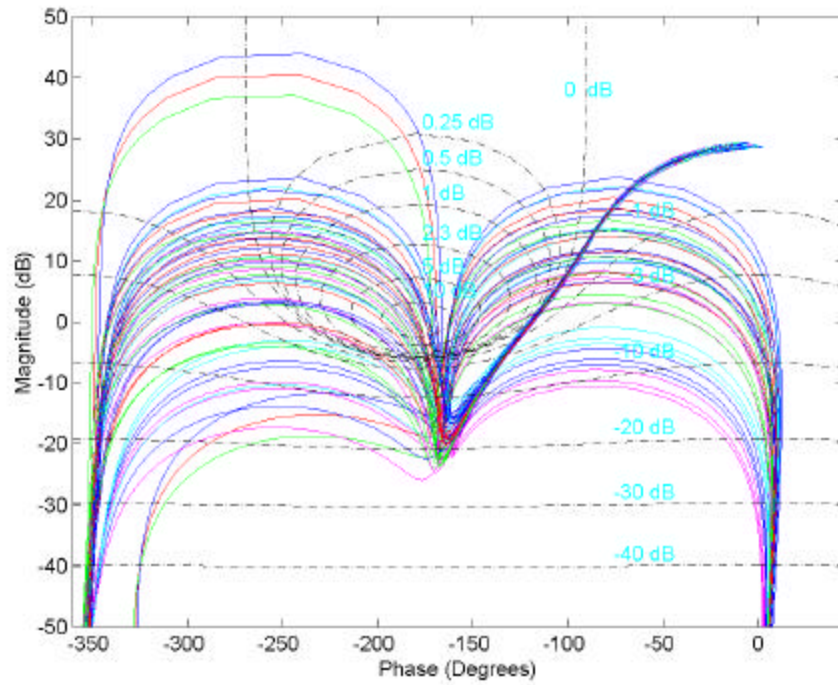


Figure 12. Nichols Plots of Uncompensated Phase Control System.

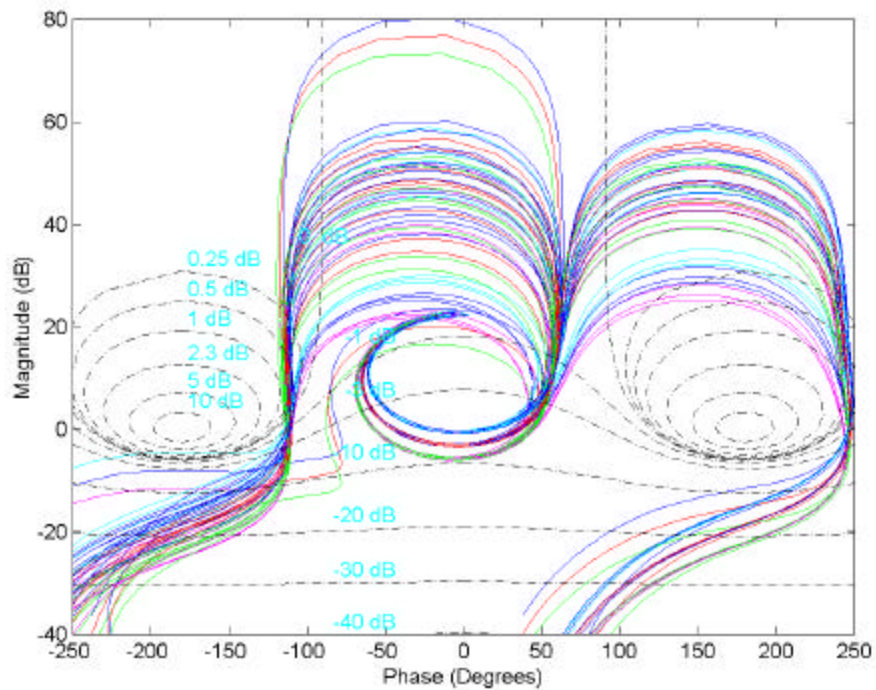
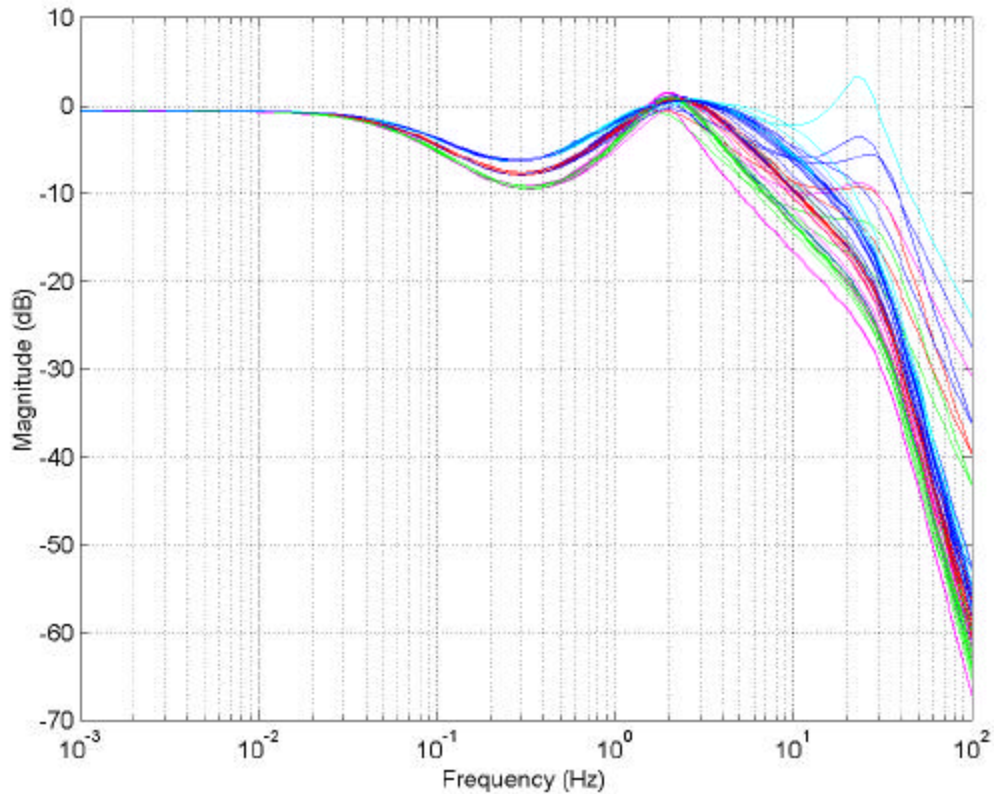


Figure 13. Nichols Plot of Compensated Phase Controller.

Because of the added nonlinearity and uncertainty of the phase control system, the original frequency control compensator  $G_2(s)$  design proved to be insufficient (with too little gain) for adequate phase control. The phase control compensator  $G_4(s)$  improved on the frequency controller and led to the new frequency control compensator  $G_3(s)$ . Since the new frequency controller has much higher gain, it has significantly better performance than the original compensator. Thus, for phase control, we have  $G_4(s) = sG_3(s)$ . The compensated phase control system is shown in Figure 13. Note that all the plants in the system have at least  $65^\circ$  of phase margin and a conditionally stable gain margin of at least  $+24/-5$  dB. Also note in Figure 13 that the circular contours that surround the  $0$  dB,  $-180^\circ$  instability point are repeated every  $360^\circ$  on the Nichols chart. Thus, the compensator design needs must not only guarantee that the system avoids the Nyquist instability point, but must also avoid the Nyquist point  $+360^\circ$ . The Bode plots of the closed-loop phase control system are shown in Figure 14.



**Figure 14. Bode Plot of Closed-Loop Phase Controller.**

## Conclusions

Quantitative feedback theory provides a simple yet powerful philosophy for designing control systems—allowing the designer to optimize the system by making design tradeoffs without getting lost in complex mathematics. The feedback systems were effective in reducing sensitivity to large and sudden changes in the power grid system. Voltage, frequency, and phase were accurately controlled, even with large disturbances to the power grid system.

Future research will apply QFT to distributive control of complex distributed generation scenarios on the power grid to minimize the effects of power transmission faults. The system will adjust power grid parameters to ensure that none of the load limits on the existing power lines are exceeded when a power line is faulted (opened). A second important direction based on this work is to directly address the issue of minimizing or eliminating reliability margins. The ultimate objective is to reach system wide coordinated real-time control.

## Distribution

1 MS0188 LDRD Program Office, 1030 (Attn: Donna Chavez)  
1 MS0501 M. K. Lau, 2338  
1 MS0501 A. E. Bentley, 2338  
1 MS0741 M. L. Tatro, 6200  
1 MS0710 A. A. Akhil, 6251  
1 MS0710 J. D. Boyes, 6251  
1 MS0451 S. G. Varnado, 6500  
1 MS0785 R. L. Hutchinson, 6516  
1 MS0785 J. E. Stamp, 6516  
1 MS0455 R. S. Tamashiro, 6517  
10 MS0455 R. E. Carlson, 6517  
1 MS0455 J. J. Torres, 6517  
1 MS9018 Central Technical Files, 8945-1  
1 MS0612 Review & Approval Desk for DOE/OSTI, 9612  
1 MS0899 Technical Library, 9616